

## A Study of the Optical and Structural Properties of the Organic Semiconductor Anthracene and Carbazole

Samah .M. Flayyih <sup>a</sup>, Abdul Hakeem Sh . Mohammad <sup>b\*</sup>, Saygin M. Nuri <sup>c</sup>

<sup>a</sup> *Department of Physics, College of Education for Pure Science, Univesity of Kirkuk, Iraq.*

<sup>b\*</sup> *Department of Physics, College of Education for Pure Science, Univesity of Kirkuk, Iraq.*

*E-mail: mohammedhassan1995130@gmail.com*

<sup>c</sup> *Department of Physics, College of Education for Pure Science, Univesity of Kirkuk, Iraq.*

---

### Abstract

This research aims to study the optical properties of anthracene and Carbazole compounds. We aim to write a comprehensive introduction to the physical properties of chains of organic compounds similar to the properties of anthracene compounds and their internal structure. We will discuss the variable absorption coefficient values according to the infrared curves and compare them with UV VIS curves. The researchers turned their attention to the coherent and characteristic structure of anthracene derivatives, which are found as building blocks based on their auto luminescent properties. The researchers [1-2-20] studied the interaction between anthracenes, Carbazole, and light. These properties include photoemission mechanisms to Designing and manufacturing organic compounds with precise properties and concentrations that contribute to many practical applications in all aspects of life. Thus, we will discuss the photo physical and structural properties of some different types of compounds and their effect on the effectiveness of light absorption, including their cohesion ability of different types of compounds for a number of samples studied in the laboratory. In this paper, we will review the most important photoelectric properties, the structure of anthracene and Carbazole compounds, and their X-ray diffraction to explore their fine structure. The results of exposing the surfaces of the samples to ultraviolet and infrared rays revealed that the absorption coefficient increases with increasing the number of strokes, and thus leads to an increase in the efficiency of the samples for use as light-emitting diodes.

**Keywords:** Optical Properties, Organic Semiconductor, Optical Energy Gap, Anthracene, Carbazole.

---

## **Introduction**

Anthracene is a very important organic compound in most electronic and electrical applications. It is also called paranthalene or green oil. Anthracene has in its structure three benzene rings ( $C_6H_6$ ) fused together in series similar to the Lewis atomic representation. Shown in Figure 1 [1-10-11]. We get anthracene from incomplete combustion reactions of fossil fuels. The International Environment Agency has given anthracene a priority and placed it at the top of its list of pollutants. Anthracene compounds are abundant in surface water, drinking water, ambient air, vehicle exhaust emissions, cigarette and cigar smoke, and in edible amphibians. Chemists have used anthracene derivatives mainly as intermediates in the production of dyes, and flash-resistance crystals, and in organic semiconductor research.

Although there is a lot of research dealing with the nomenclature of polycyclic aromatic hydrocarbons, these nomenclatures are limited when it comes to anthracene compounds. On the other hand, Carbazole derivatives have gained much interest from medicinal chemists by researchers for many decades because these compounds have a wide range of biological and pharmacological properties. The important properties of anthracene and Carbazole compounds lie in their antibacterial, antitumor, antioxidant, and anti-inflammatory activities. [4-5-18]

The natural, semi-synthetic or synthetic therapeutic properties of Carbazole-containing molecules have been highly acclaimed for their essential an essential role in detecting symptoms and development of diabetes. Many studies have confirmed the importance of Carbazole derivatives in reducing oxidative stress; prevent adrenergic hyperactivity, In addition to preventing damage to pancreatic cells and modulating carbohydrate metabolism. In this paper, we will summarize the most important and recent developments in synthetic and natural Carbazole-containing compounds and their optical properties [2-3-12]

Organic semiconductor compounds are among the most widely used compounds in electronic fields due to their low cost, lightweight, and good solubility. The physical and chemical properties of these compounds can be modified by chemical composition and recrystallization. , and this is what makes it the focus of attention of most researchers because it deals with photovoltaic solar cells, and organic light-emitting diodes [3-4-14]. These materials have attracted great attention in the field of biosensors in recent decades and have been used in medical diagnosis and personal safety, and a gas sensor that operates because of modulation of electrical properties.

The importance of studying these compounds and knowing their properties lies in the possibility of determining the amount of oxygen, which has a major role in health processes and disease treatment [3.5]. The researchers found composite chains of (LED) based on the fusion of anthracene and Carbazole derivatives.

These compounds have shown deep blue emission in literature. The brightness and current efficiency characteristic of these composites described as OLED did not reach high values [22-23-24]. By studying the properties of blue anthracene-derived compounds (LED), chemists have noted the difficulty in achieving other accompanying features (such as High fluorescence, large current conductivity, photoemission-dependent conductivity, and good mechanical structure). However, the scientists were unable to find out the effect of the organic side chains on the EL properties of the anthracene derivatives. Therefore, it is important to carry out more research that includes studying the effect of organic chains and structures of anthracene derivatives on physical properties and electrochemical behavior [3-6-7-15]. The strength, melting point and hardness of organic compounds can be improved by incorporating the Carbazole moiety into an organic macromolecular compound [5]. We can easily synthesize three or six classes of Carbazole moiety compounds, We can tune the photoelectric properties of the particles in the surface layers of the prepared samples. We have synthesized a series of anthracene derivatives linked to the Carbazole moiety for use as light emitters Diode in LED. Figure (1) it shows the structure of the chemical compounds derived from the group of Carbazole compounds related to the derivatives of anthracene compounds

Later, chemists attempted to synthesize a series of anthracene-related Carbazole derivatives for use as light-emitting diodes (LED) [5]. Figure 1 shows the chemical structures of the Carbazole moieties fused to anthracenes. The EL properties of anthracene derivatives or anthracene-like LED contain only moderate bonds; the reason for these properties is due to the weak coupling of anthracene derivatives attached to moieties of anthracene compounds. Lateral co-chain bonds negatively affect the physical properties of the mechanical structure and electrochemical behavior of blue light-emitting diodes, and thus led to a weakening of the EL performance of the LED screens. Nevertheless, we seek through these researches and the study of the optical and structural properties in order to obtain coupling with stronger and more optically efficient co-ligands.

We have synthesized and studied simple sequences Anthracene, substituted anthracene derivatives and some Carbazole compounds include side moieties and organic chains containing ethylene, Carbazole, and anthracenes. We have studied the UV curves with the aim of employing them as light emitting Diode (LED), the location of the

Carbazole groups on positions of the C9 and C10 groups of the anthracene unit. We analyzed the effect of Carbazole and anthracene moieties and their corresponding adsorption coefficients on thermal stability, structural properties and physical behavior, ending with the performance Devices containing anthracene derivatives. The process of determining the percentage of oxygen in these organic compounds plays an effective role in the fields of health and disease treatment [5-8]. These industrial areas require sophisticated sensors that operate at lower temperatures [6]. The effective of conventional resistive gas sensors based on inorganic semiconductors such as TiO<sub>2</sub> decreases with high temperature, so it can be considered as a negative factor in determining gravimetric ratios. The academic community has delved into the chemical and pharmacological properties of Carbazole-containing heterocyclic molecules. The increasing interest in these derivatives has led to the development of different methods as well as their extraction from different plants. Scientists have found many Carbazole-containing molecules that can be used in the medical field.

The studies included in this paper showed that some Carbazole and anthracene derivatives are important antidiabetic agents.

These studies aim at the possibility of obtaining coupling with more efficient and stronger co-ligands of the C3 group when associated with molecules of Carbazole compounds in C9 and C10 sites of anthracene unit.

## Experimental Section

### Materials and General Methods

Figure 1 and Figure 2 shows the molecular structure of anthracene and Carbazole. According to Schiff's rule, we studied these synthesized compounds and compared the properties for each sample [7-16-17-25-24]. In this research, we used organic compounds derived from anthracene and Carbazole, namely Vitalic anhydride (99%, Sigma-Aldrich), anthracene (98%, Acros), Sodium aside (99.5%, Sigma), Propargylic alcohol, sodium ascorbate (98%, Sigma).

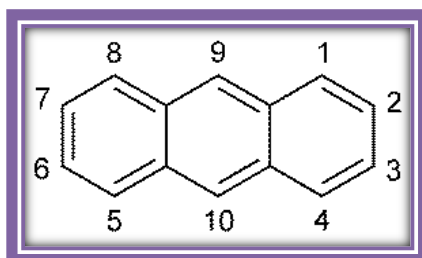


**Fig. 1: Shows the Molecular Structure of Anthracene**

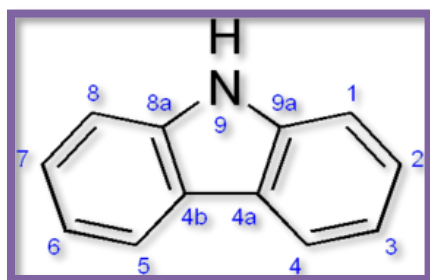


**Fig. 2: Shows the Molecular Structure of Carbazole**

### Devices and Tools Used

We explored several properties of anthracene and Carbazole compounds using a Cary 2300 UV-vis spectrophotometer. We periodically checked and observed the electrical measurements of DC and AC current in a custom vacuum dark cell using a Keithley 236 source measurement unit. We conducted the tests using a fully automated experimental setup developed as shown in Fig. 2. We used nitrogen as an equilibrium with a flow of 100 NL h<sup>-1</sup> and obtained the required test gas concentration using a volumetric flow controller. The sensor consisted of a glass substrate and an ITO anode, on top of which we deposited a thin film using an appropriate coating. We were able to deposit the metal cathode on the aluminum element with the heat of vaporization by the high vacuum technique [17-18].

## Results and Discussion

### Optical Measurements

#### Optical Absorbance

We studied the optical properties of Carbazole and anthracene films for each of the three prepared samples, and we recorded the results and comparing the absorption spectra as a function of the photon energy for each sample according to the visible (VIS) and ultraviolet (UV) range 190-2100 nm. We analyzed and compared the absorption spectra for each sample, then calculated the forbidden energy gap for the allowed direct electron transitions.

#### Absorbance Spectra for Carbazole Samples

Figure 3 It shows the changing absorption spectra as a function of wavelength for the three-Carbazole samples. The absorption has a maximum value at the main absorption edge (short wavelengths), and absorption values are in the range (200-400nm), within the ultraviolet field region.

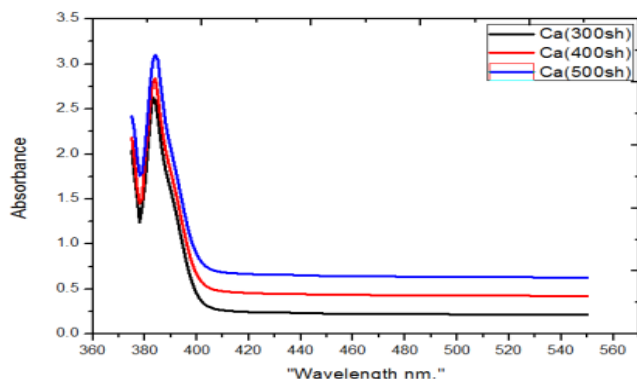


**Fig. 3: Shows the Absorbance Values as a Function of Wavelengths for Carbazole Samples**

We notice that the absorptivity values decrease with increasing length of the wave, which confirms physically that the energy of the incident photon, is small compared to the energy of the electron in its orbit, and therefore the photon can no longer excite the electron and transfer it from the valence band to the conduction band. The number of strokes affects the absorbance values through their correlation with the wavelength, as the absorbance increases when the number of strokes increases.

#### Absorption Spectra of Anthracene Samples

Figure 4 shows the change of the absorbance spectrum as a function of the wavelength of the three-anthracene samples. The absorbance reaches its greatest value at the main absorption edge (short wavelengths), and the absorption values are in the range (200-400nm), within the ultraviolet field region. We can use anthracene compounds as gradients or sensors in many applications such as photoluminescence, metal ion detection, intracellular pH sensing and DNA binding sensing, and thus we conclude that the absorbance values decrease with increasing wavelength [19-20-21].

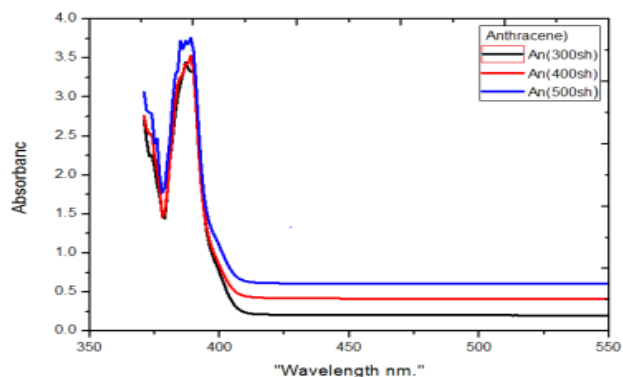


**Fig. 4: Shows the Absorbance Values as a Function of Wavelengths for Anthracene Samples**

Figure shows that the energy of the incoming photon is small, which makes it unable to excite the electron and transfer it from the valence level to the conductive level. On the other hand, the energy of the incoming photon is less than the energy gap in semiconductors, so the absorbance decreases with increasing wavelength. Based on the foregoing, the values of the absorbance coefficient at the same wavelength are directly proportional to the number of strokes. The difference between the samples is very small, and therefore the absorption coefficient increases when the number of hits on the samples increases because of the increase in the number of particles inside the sample, as their ability to absorb more incoming ray's increases.

### Absorbance Coefficient

We determined the optical gap energy using the Tauc method [8] which states that the adsorption coefficient ( $\alpha$ ) represents the mutual interaction between Photon energy and energy gap  $E_g$  according to the following relationship:

$$E = A(Hv - E_g)(\alpha hv)^n \quad (1 - 1)$$

Conventionally, it takes ( $n$ ) to be the value (1/2) when determining gap energy of an organic semiconductor [23]. The energy gap corresponds to the point of intersection separating the extrapolation of the linear part from the ordinate axis.

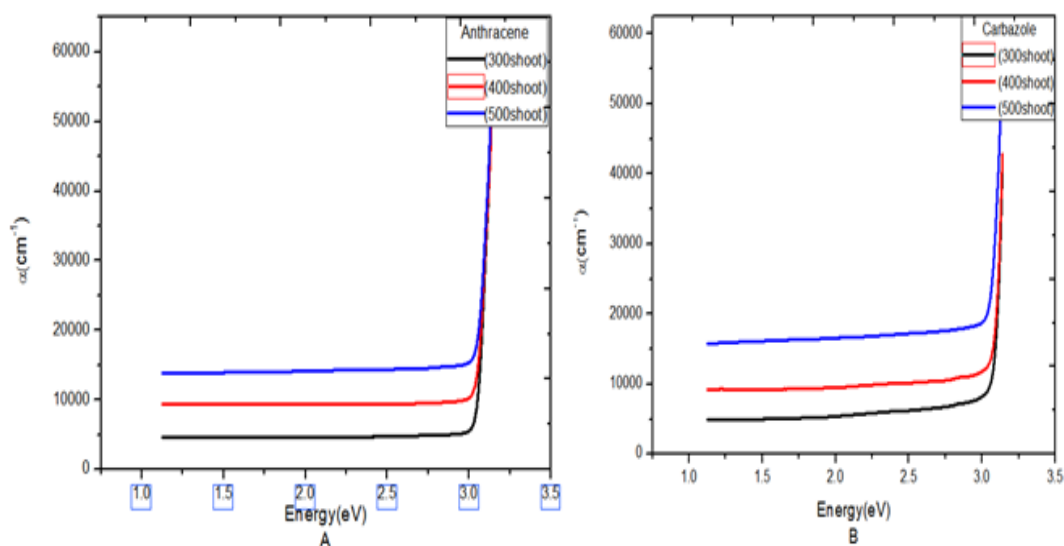


**Fig. 5: Absorption Coefficient Variation as a Function of Photon Energy for Carbazole and Anthracene Films**

Figure 5 shows the values of the absorption coefficient, which we calculate as a function of the photon energy corresponding to the films of different Carbazole and anthracene compounds. The Carbazole curves show that the absorption coefficient rises with the energy of the incoming photon [23-24-25].

We notice a similarity in the behavior of the absorption coefficient curves for all the prepared films, as they reach close values up to 17000cm in Figures 5-6, then the absorption coefficient values begin to increase when the energy of the incoming photon reaches 3eV. Figure 5 shows that the value of the absorption coefficient for the third sample of Carbazole exceeds that of the first and second samples when the energy of the incoming photon is increased, and this is due to the fact that the third sample has a larger number of molecules that enable it to have a higher absorption capacity for rays due to the increase in the number of hits, and this is what we find similarly in Figure 4.

### Optical Band Gap

We calculated the optical energy gap corresponding to the allowable transitions of electrons for Carbazole and anthracene films, we used the relationship considering  $r = 1/2$ , then we drew the linear relationship that describes the changes of  $\alpha hv$  depending on the energy of the incoming photon  $Hv$ . We extend the straight part of the axis to cut the energy axis of the photon so that the relationship used 1-1 is achieved when  $(\alpha hv)^2 = 0$ .

on the other hand, then  $E = E_g = hv$ , We conclude that the cut-off point of the axis represents the value of energy gap for the allowed direct transmission  $E_{g\ opt}$ .

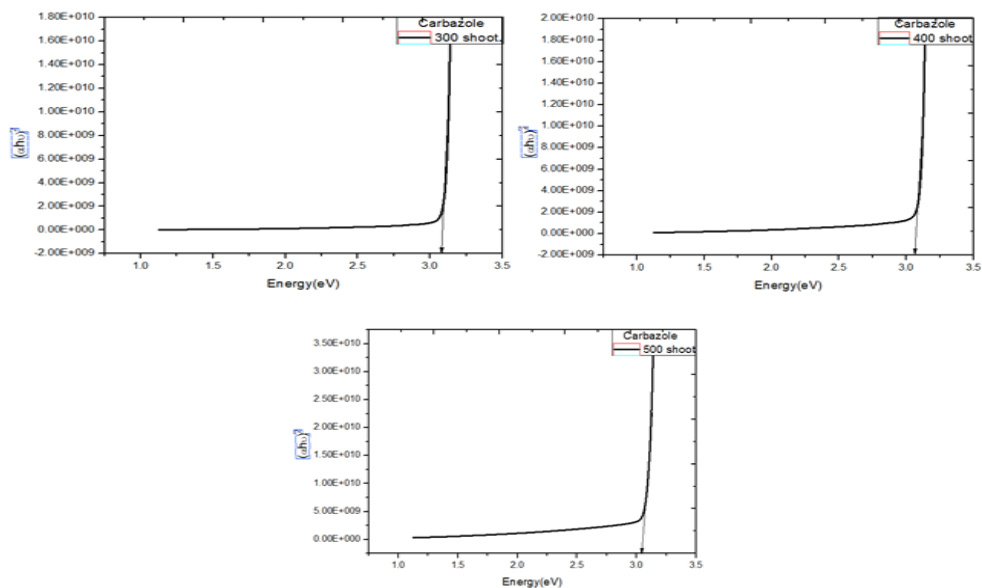


**Fig. 6: Optical Energy Gap as a Function of Incident Photon Energy for Carbazole Films for Three Prepared Samples**

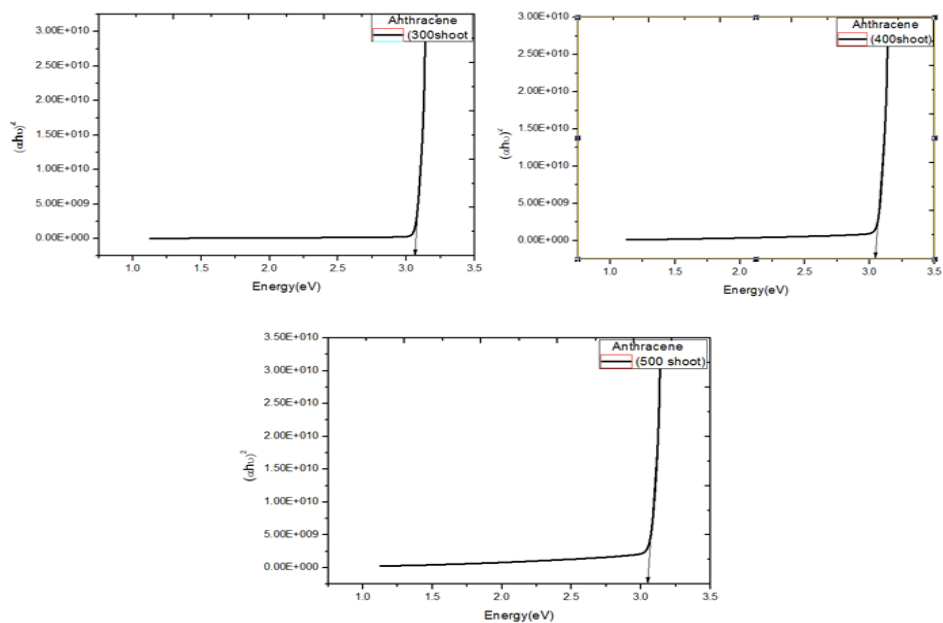


**Fig. 7: Optical Energy Gap as a Function of Incident Photon Energy for Anthracene Films for Three Prepared Samples**

Figures 6.7 show a decrease in energy gap values, reaching 3.09035 eV, with close values for the Carbazole and anthracene membranes. The reason for this decrease is due to the increase in the number of blows or the amount of material, which in turn leads to the displacement of the range of valence and conductivity levels, depends on the increase in the sizes of molecules within the membranes of the compounds.

### Transmittance

We calculated the permeability coefficient, as Figure 14 shows a graph opposite the absorbance curve, showing that the permeability of Carbazole and anthracene membrane compounds is low at the main absorption edge. Transmittance rises with increasing wavelength or increases with decreasing energy and a sudden increase appears until it stabilizes in the visible region of wavelengths.

We notice a decrease in the permeability when the number of hits is increased for the samples prepared for Carbazole and anthracene films, the permeability takes a lower value for the samples that have a greater number of hits (500 hits) as shown in the following figure 8.

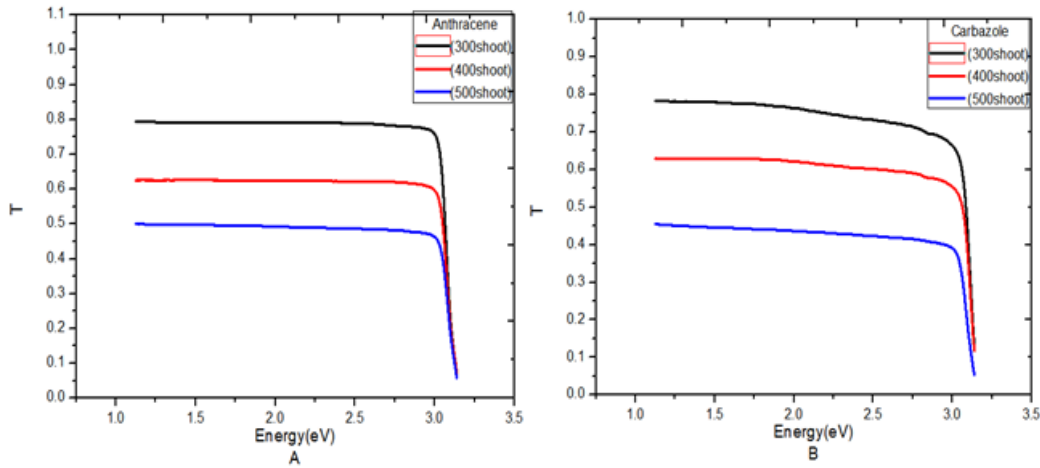


**Fig. 8: Shows the Values of Permeability as a Function of Energy for Carbazole and Anthracene Films**

**Urbach Energy**

We have many ways to absorb rays for semiconductors; we calculated Urbach energy for Carbazole and anthracene films by calculating the inverse regression  $\ln\alpha$  as a function of photon energy.

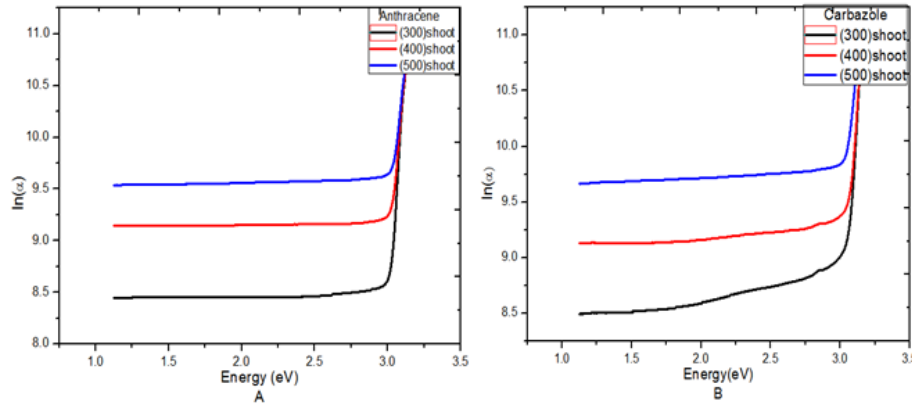


**Fig. 9: Shows the Urbach Energy for the Carbazole and Anthracene Membranes for the Six Different Samples Prepared by the Number of Strokes**

The figure 9 shows the decreasing energy of Urbach with the increase in the number of blows inside the samples, as it leads to an increase in the number of molecules that makes them absorb more energy than the incoming rays, which increases the energy of the optical gap, as the energy of Urbach 3eV reached according to an inverse regression coefficient that ranged between

We note that the optical behavior of the Urbach energy is completely opposite to the optical behavior of the optical gap energy, which confirms that the crystals crystallize well when they absorb the incoming rays.

**Extinction Coefficient**

The passivity coefficient determines the extent to which a material absorbs or reflects incoming radiation at a given wavelength. We calculated the quenching coefficient for all samples prepared for Carbazole and anthracene using the relation:

$$k = \frac{\alpha\lambda}{4\pi} \quad (2 - 2)$$

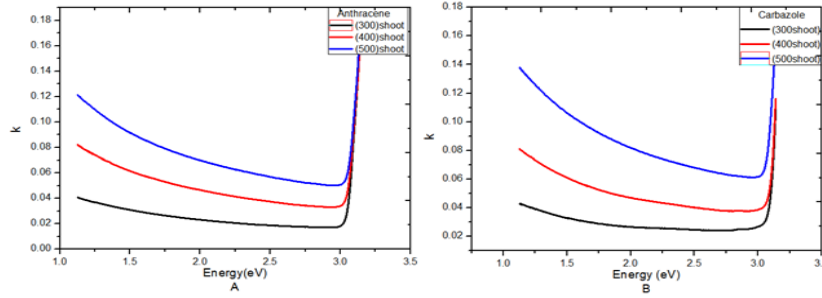


**Fig. 10: Shows Inertia Coefficient of Carbazole and Anthracene Thin Films**

**Figure 10** shows a great similarity in the values of the quenching coefficient for the films of Carbazole and anthracene, we notice a decrease in the quenching coefficient at long wavelengths, as it takes values ranging from  $k = 0.05 - 0.15$  Wavelengths range from 400 to 500nm. We conclude from the foregoing that the damping coefficient takes its greatest value at short wavelengths, and this confirms the importance of increasing the number of hits in the prepared samples, which increases the levels of the conduction band, which is directly related to the absorption coefficient.

### Refractive Index

We calculated the refractive index and noticed a similarity between the refractive index and the reflectivity coefficient, which increases when the waveforms and the number of atoms increase in the samples prepared for Carbazole and anthracene films as shown in the following figure11.

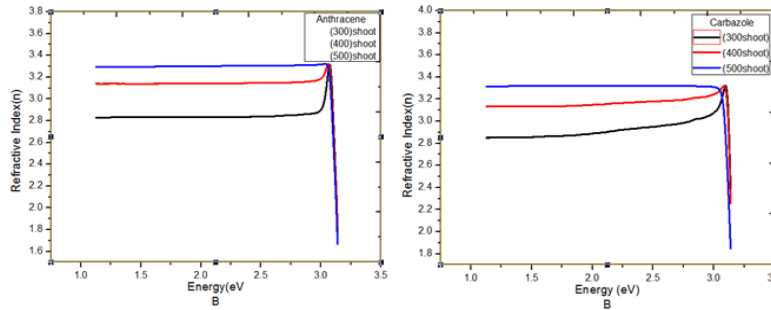


**Fig. 11: The Figure Shows the Refractive Index of Carbazole and Anthracene Films**

We conclude from Figure 11 that the refractive index is directly related to the increase in the number of strokes. This increase is attributed to the increase in the packing density and the change in the crystal structure of the samples prepared at short wavelengths.

### Optical Conductivity

We calculated the optical conductivity as a function of the photon energy for all the prepared films. Figure 12 shows the increase of the optical conductivity according to the increase of the photon energy. We notice a decrease in the conductivity value when the thickness is reduced

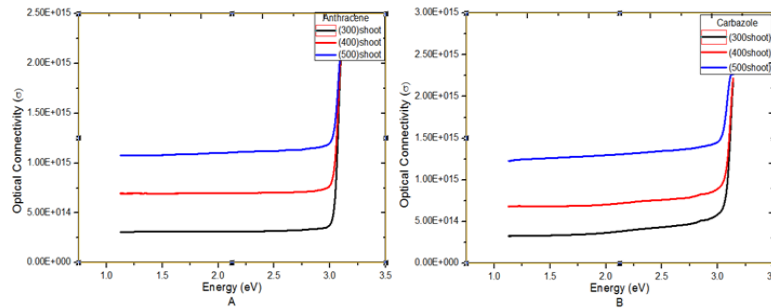


**Fig. 12: It Shows the Optical Conductivity of Differently Prepared Carbazole and Anthracene Films by the Number of Strokes**



### Experimental FT-IR Spectra Curves

The FT-IR spectra curves show the peaks indicating the high and low absorption coefficients of the anthracene derivatives. We improved these compounds by incorporating a phenyl ring between the Carbazole and anthracene groups. On the other hand, we noticed a similarity between the absorption coefficient values of some anthracene derivatives with Carbazole derivatives.

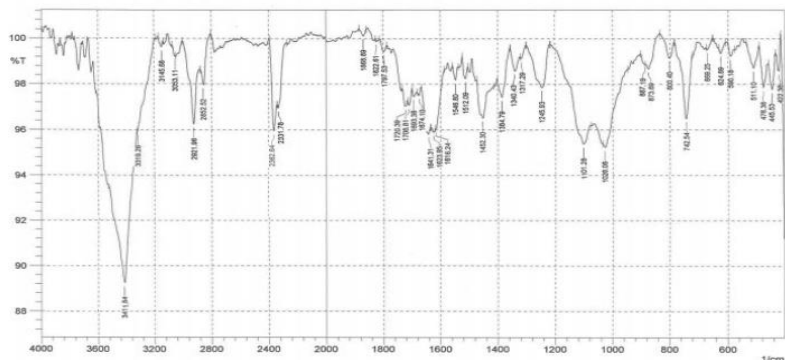


Fig. 13: FT-IR Spectra Curves of the First Carbazole Sample

Figure 13 shows the curves of the experimental **FT-IR spectra**, which show the change of the absorption coefficient for the first sample of Carbazole derivatives, which shows the changes of the peaks values of the absorption coefficient in terms of depth, the figure shows the presence of two main peaks, three main peaks at  $3415.70$  and  $3001.91\text{ cm}^{-1}$ . The compatibility of the absorption rate ranges between 80-90%.

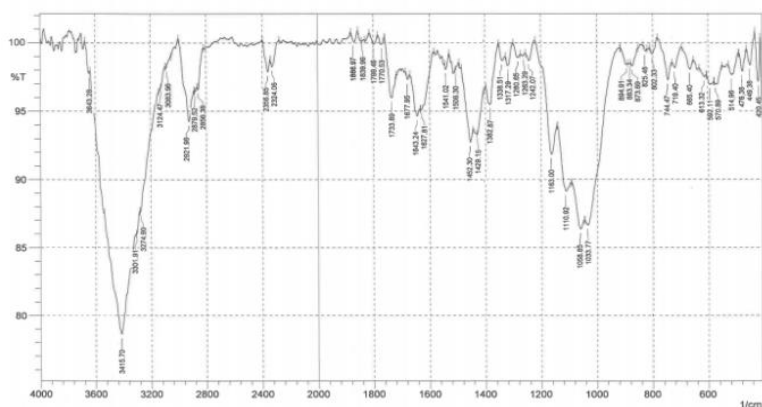


Fig. 14: FT-IR Spectra Curves of the Second Carbazole Sample

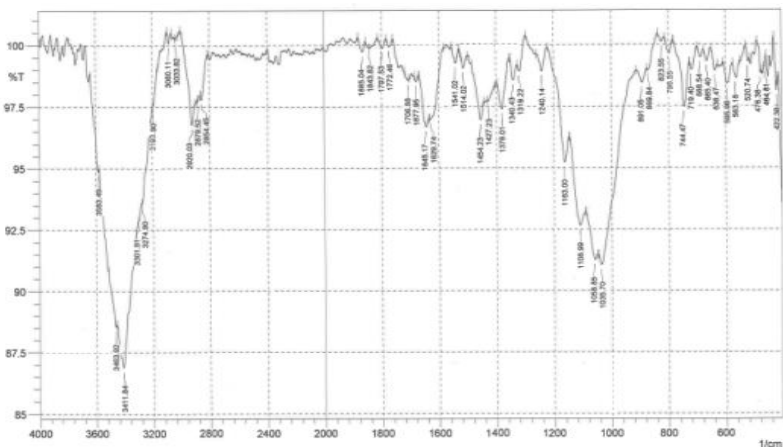
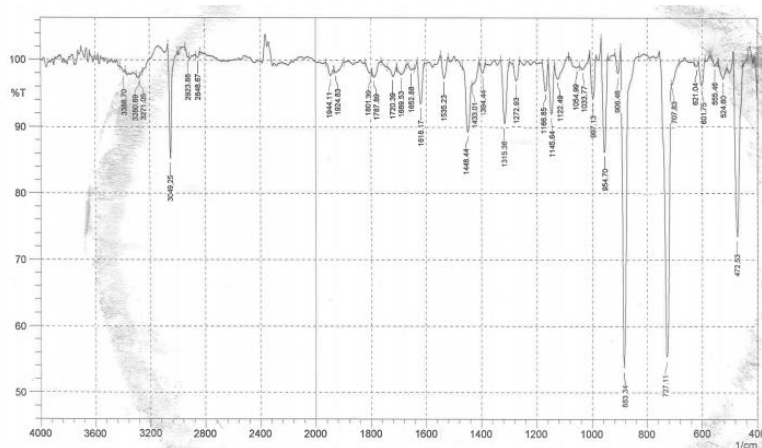
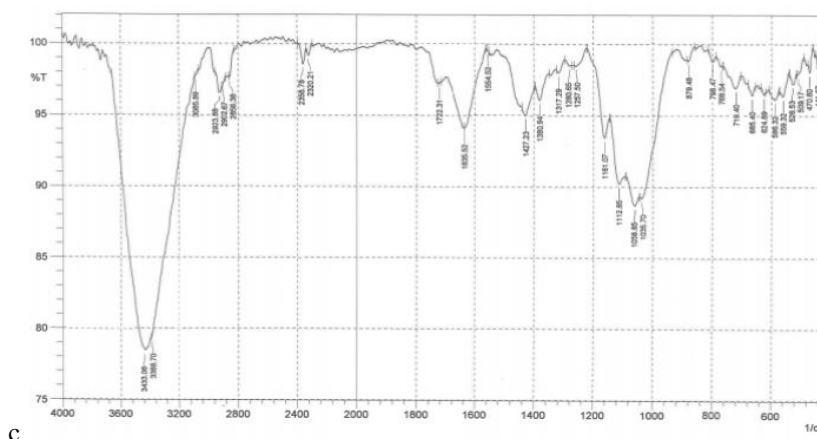


Fig. 15: FT-IR Spectra Curves of the Third Carbazole Sample

**Figure 14-15** the curves of the experimental spectra for the second and third Carbazole samples, which increase the number of strikes from the first sample shown in form 7, shows the changes in the values of the absorption coefficient in terms of depth, and the two forms show the presence of two main major summits that range in the values of the absorption coefficient for them. Between  $(1008-1185.70) \text{ cm}^{-1}$  to become low value for the absorption laboratory  $3411.84 \text{ cm}^{-1}$  85 %absorption rate, due to the high number of strikes, which in turn increases absorption values.



**Fig. 16: FT-IR Spectra Curves of the First Anthracene Sample**



**Fig. 17: FT-IR Spectra Curves of the Second Anthracene Sample**

We note from Figures 16-17 the curves of the experimental **FT-IR spectra** for the two-anthracene samples, showing changes in the values of the absorption coefficient in terms of depth. The three figures show the presence of close main peaks ranging from The values of the absorbance coefficient are between  $1058-1112.85 \text{ cm}^{-1}$  while they have low rates of the absorbance coefficient corresponding to the lower peak of  $3433.83 \text{ cm}^{-1}$  The reason is due to the high number of strokes, which in turn increases the absorbance values.

We conclude from the previous two figures that there are almost similar peaks, and the reason is that the two samples of anthracene have a large number of particles because of the increase in the number of hits, which increases the value of the absorption coefficient of the incoming rays.

The FTIR spectra curves (Fig. 16) show absorption bands corresponding to  $\text{C} = \text{N}$  with an average value of approximately  $(2800-3049 \text{ cm}^{-1})$ , while the methylene bonds are characterized by an absorption coefficient value of  $\text{N}-\text{C} = \text{S}$   $(1448.44 \text{ cm}^{-1})$ . The absence of an  $\text{S} - \text{H}$  vibration band at  $418 \text{ cm}^{-1}$  and the presence of bands due to a  $\text{C} = \text{S}$  vibration at  $(555.46 \text{ cm}^{-1})$  confirm that the  $\text{CS}$  group is still in thion form [7-8]. We analyzed the

The curves show the FT-IR spectra of the compounds of anthracene and Carbazole derivatives  $(4000-500 \text{ cm}^{-1})$ . The chains of bonds represented by the characteristic peaks of  $\text{C} = \text{N}$  and  $\text{C} = \text{S}$  take values of lower wavelength. On the other hand, the vibrations related to the common  $\text{N}-\text{C} = \text{S}$  chains take values with higher wavenumbers in all metallic derivatives and compounds (Table 2). These changes support the  $\text{C}=\text{N}$ ,  $\text{N}-\text{C}=\text{S}$ , and  $\text{C}=\text{S}$  vibrations.

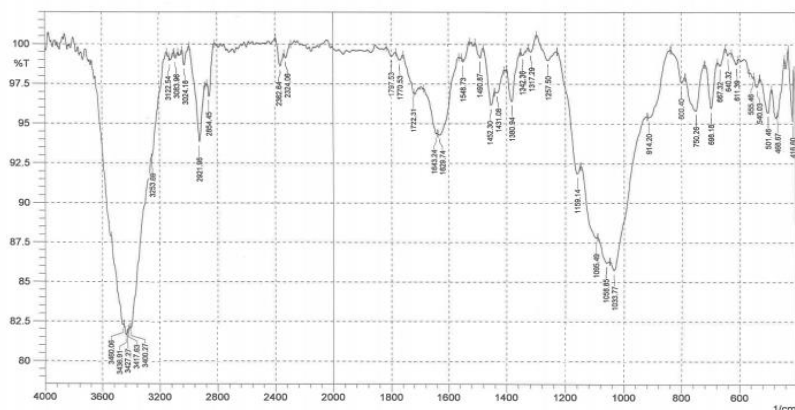


**Fig. 18: Experimental FT-IR Spectra Curves for the Third Sample of Anthracene**

Characterization of the FTIR spectra Figure (15-16-17) shows peak values corresponding to C = N, low absorption values for anthracene and Carbazole compounds, which indicates the presence of dense and close absorption bands with C = N bond values, the absorption peak has a maximum value of approximately  $3049.25\text{cm}^{-1}$ .

Characterization of the FTIR spectra Figure (16-17) shows peak values corresponding to C = N, high absorption values for anthracene and Carbazole compounds, which indicates the presence of dense and close absorption bands with C = N bond values, the absorption peak has a maximum value of approximately  $(2800-3200)\text{cm}^{-1}$ .

We concluded from the spectral characterization according to the IR curves that most of the bonds of Carbazole and anthracene compounds are characterized by somewhat close absorption values and their intensity increases due to the presence of double bonds (C - N) and C=CH<sub>2</sub>, and this confirms the importance of these compounds in electronic uses And electric energy tanks and can be used later in the fields of solar energy.

## Conclusions

We have definitively defined the properties of Carbazole and anthracene derivatives, and performed structural characterizations of the compounds using elemental analyses, spectroscopic method curves, Structural and conductive studies and thermal analysis. We concluded from the spectral characterization according to the infrared curves and the UV VIS curves that most of the bonds of Carbazole and anthracene compounds are characterized by fairly close absorption values and their intensity increases due to the presence of double bonds (C - N) and C=CH<sub>2</sub>, and this confirms the importance of these compounds in electronic uses and energy storages It can be used later in the fields of solar energy. We have proven that increasing the number of atoms on the samples increases the number of molecules stationed within the surface layer, which makes them more capable of absorbing the incoming photon rays, and this in turn allows the largest number of high-energy photons to reach a depth Diffusion layer, thus increasing the number of removed electrons

## Reference

- Nie, F., Cui, Z., Bai, F., & Wang, Z. (2019). Properties of solid particles as heat transfer fluid in a gravity driven moving bed solar receiver. *Solar Energy Materials and Solar Cells*, 200.
- Tang, C.W. (1989). VanSlyke SA and Chen CH. *Journal of Applied Physics*.
- Azrain, M.M., Mansor, M.R., Fadzullah, S.H.S.M., Omar, G., Sivakumar, D., Lim, L.M., & Nordin, M.N.A. (2018). Analysis of mechanisms responsible for the formation of dark spots in organic light emitting diodes (OLEDs): A review. *Synthetic Metals*, 235, 160-175.
- Raijmakers, L.H.J., Büchel, M., & Notten, P.H.L. (2018). Impedance-based temperature measurement method for organic light-emitting diodes (OLEDs). *Measurement*, 123, 26-29.
- Joule, J.A. (1984). *Adv Heterocyclic Chem* 35: 83 und dort zit.
- Park, J.S., Park, C.O., Kim, H.J., & Miura, N. (2005). Low temperature oxygen sensor using YSZ|  $\beta$ -  $\beta$  "alumina bioelectrolyte. *Solid State Ionics*, 176(15-16), 1371-1375.
- Zhang, Y., Mali, B.L., & Geddes, C.D. (2012). Metal-enhanced fluorescence exciplex emission. *Spectrochimica Acta Part A: Molecular and Biomolecular Spectroscopy*, 85(1), 134-138.

- Chen, L.Y., Shiu, Y.J., Wu, Y.J., & Huang, W.Y. (2020). Simple structured color tunable white organic light-emitting diodes utilizing an ambipolar anthracene derivative with low-lying LUMO. *Organic Electronics*, 76.
- Bowen, E.J. (1954). Fluorescence quenching in solution and in the vapour state. *Transactions of the Faraday Society*, 50, 97-102.
- Labianca, D.A., Taylor, G.N., & Hammond, G.S. (1972). Structure-reactivity factors in the quenching of fluorescence from naphthalenes by conjugated dienes. *Journal of the American Chemical Society*, 94(11), 3679-3683.
- Weller, A.L.B.E.R.T. (1968). Electron-transfer and complex formation in the excited state. *Pure and Applied Chemistry*, 16(1), 115-124.
- Ohshiro, I., Ikegami, M., Nishimura, Y., & Arai, T. (2006). Exciplex formation of intermolecularly hydrogen-bonded system between anthracene and N, N-dimethylaniline derivatives. *Bulletin of the Chemical Society of Japan*, 79(12), 1950-1954.
- Yang, N.C., Shold, D.M., & Kim, B. (1976). Chemistry of exciplexes. 5. Photochemistry of anthracene in the presence and absence of dimethylaniline. *Journal of the American Chemical Society*, 98(21), 6587-6596.
- Yang, N.C., Shold, D.M., & McVey, J.K. (1975). Chemistry of exciplexes. III. Exciplex fluorescence from anthracene and substituted anthracenes in the presence of 2, 5-dimethyl-2, 4-hexadiene. *Journal of the American Chemical Society*, 97(17), 5004-5005.
- Mizuno, K., Pac, C., & Sakurai, H. (1974). Photochemical reactions of aromatic compounds. XIX. Photocycloaddition of olefins to 9-cyanophenanthrene. Singlet exciplex or triplet mechanism depending on olefins. *Journal of the American Chemical Society*, 96(9), 2993-2994.
- Cann, J.R., Cabanetos, C., & Welch, G.C. (2018). Synthesis of Molecular Dyads and Triads Based Upon N-Annulated Perylene Diimide Monomers and Dimers. *European Journal of Organic Chemistry*, 2018(48), 6933-6943.
- Birks, J. B. (1975). Excimers. *Reports on progress in physics*, 38(8).
- Bureš, F. (2014). Fundamental aspects of property tuning in push-pull molecules. *Rsc Advances*, 4(102), 58826-58851.
- Brunner, K., Van Dijken, A., Börner, H., Bastiaansen, J.J., Kiggen, N.M., & Langeveld, B.M. (2004). Carbazole compounds as host materials for triplet emitters in organic light-emitting diodes: tuning the HOMO level without influencing the triplet energy in small molecules. *Journal of the American Chemical Society*, 126(19), 6035-6042.
- Matteucci, E., Baschieri, A., Sambri, L., Monti, F., Pavoni, E., Bandini, E., & Armaroli, N. (2019). Carbazole-Terpyridine Donor-Acceptor Dyads with Rigid  $\pi$ -Conjugated Bridges. *ChemPlusChem*, 84(9), 1353-1365.
- Ge, J.Z., Zou, Y., Yan, Y.H., Lin, S., Zhao, X.F., & Cao, Q.Y. (2016). A new ferrocene-anthracene dyad for dual-signaling sensing of Cu (II), Hg (II). *Journal of Photochemistry and Photobiology A: Chemistry*, 315, 67-75.
- Hauschild, M., Chen, L., Etschel, S.H., Ferguson, M.J., Hampel, F., Halik, M., & Tykwinski, R.R. (2020). Anthracene-Pentacene Dyads: Synthesis and OFET Characterization. *ChemPlusChem*, 85(5), 921-926.
- Etschel, S.H., Margraf, J.T., Amin, A.Y., Hampel, F., Jäger, C.M., Clark, T., & Tykwinski, R.R. (2013). An unsymmetrical pentacene derivative with ambipolar behavior in organic thin-film transistors. *Chemical Communications*, 49(60), 6725-6727.
- Parada, G.A., Goldsmith, Z.K., Kolmar, S., Pettersson Rimgard, B., Mercado, B.Q., Hammarström, L., & Mayer, J. M. (2019). Concerted proton-electron transfer reactions in the Marcus inverted region. *Science*, 364(6439), 471-475.
- Ariga, K., Hill, J. P., Lee, M. V., Vinu, A., Charvet, R., & Acharya, S. (2008). Challenges and breakthroughs in recent research on self-assembly. *Science and technology of advanced materials*.